

Template Control Preparation of High-Density and Large-Area Ag Nanowire Array and H₂O₂ Determination

Min Zhang, Yan Zhang, Peng Liu, Meiqiong Chen, Zhiquan Cai, Faliang Cheng*

Dongguan University of Technology, Guangdong Engineering and Technology Research Center for Advanced Nanomaterials, Dongguan, Guangdong, 523808, China

*E-mail: chengfl@dgut.edu.cn

Received: 23 December 2014 / Accepted: 1 March 2015 / Published: 23 March 2015

Highly ordered Ag nanowire arrays were prepared by template-electrodeposition method using anodic aluminum oxide template. The length of Ag NW arrays were controlled by electrodeposition time and characterized by scanning electron microscope (SEM) and Energy Dispersive Spectrometer (EDS). Different length Ag NW arrays modified electrodes for H₂O₂ detection were studied by cyclic voltammetry (CV). The results showed that the about 250 nm length Ag NW arrays exhibited the highest electrocatalytic activity for H₂O₂ with a wide linear range (1 to 750 μM), low detection limit (0.28 μM) (S/N = 3) and short response time (within 3 s). The proposed sensor had high sensitivity (13.4 μA mmol⁻¹L cm⁻²). The sensor also had good selectivity toward H₂O₂ in the presence of electrochemical interferences such as ascorbic acid, uric acid and glucose.

Keywords: Ag NW arrays, Template control preparation, H₂O₂ determination

1. INTRODUCTION

H₂O₂, one of the powerful oxidation reagents, can be applied as disinfection, sterilization, albefaction and so on in chemical industry, textile industry, papermaking, food, medicine, electron field and environmental protection. Hence, it is important for developing rapid, sensitive methods to monitor trace levels of H₂O₂ concentration. Various analytical methods, such as photometric, [1-3] chromatographic [4] and electrochemical method [5-9] have been reported to determine H₂O₂. Compared with spectroscopic analysis and chromatographic determination, sensors have merit of low cost, simplicity, sensitivity and present-operation. With superior characteristic, sensors were widely applied for determination H₂O₂ concentration.

Metal nanomaterials explored as electrochemical interface will provide a very high electrochemically active area, a rapid electron transfer rate and thereby lead to high detection

sensitivity[10-15]. Compared with other metal nanomaterials, silver may facilitate more efficient electron transfer due to the highest conductivity. The sensors based on silver nanomaterial were broadly researched. For instance, Qin, et al. [5] reported on preparation of Ag NPs-decorated polypyrrole colloids (Ag NPs-PPyCs) by heating an AgNO₃ aqueous solution and pre-formed PPy colloids solution in the presence of any external reducing agent. The sensor showed a fast amperometric response time less than 2s, and the corresponding linear range and detection limit were estimated to be from 0.1 mM to 90 mM and 1.05 μM. Li et al. [16] prepared a novel amperometric biosensor based on AgNPs/MWCNTs-IL modified glass carbon electrode. The constructed electrode exhibited good catalytic activity toward the reduction of H₂O₂, and obtained a linear response to logarithm of the H₂O₂ concentrations ranging from 1.2×10^{-8} to 4.8×10^{-6} M with a limit of detection (LOD) of 3.9×10^{-9} M. Lu, et al. [17] introduced the first preparation of well-defined SiO₂-coated grapheme oxide (GO) nanosheets without prior GO functionalization by combining sonication with sol-gel technique. The functional SiO₂/GO nanocomposites obtained by surface functionalization with NH₂ group were subsequently employed as a support for loading Ag nanoparticles to synthesize AgNPs/F-SiO₂/GO. The prepared sensor had a fast amperometric response time of less than 2 s. The linear range was estimated to be from 0.1 to 260 mM and the detection limit was estimated to be 4 μM.

Although enzymatic sensors exhibit high sensitivity and good selectivity, they often suffer from chemical and thermal instabilities, because the activity of enzymes is easily affected by temperature, pH-value, humidity and toxic chemicals. The non-enzymatic sensors were prepared to solve this problem. Jamal et al. [18] reported a non-enzymatic amperometric H₂O₂ sensor based on Pd nanoparticle modified gold nanowire array electrode. The sensor showed a linear response up to 2 mM of H₂O₂ with a sensitivity of 530 μA mM⁻¹ cm⁻². Huang et al. [19] introduced a novel non-enzymatic H₂O₂ biosensor based on the CuO-SiNWs electrodes. The resulted sensor exhibited excellent performance for H₂O₂ determination with a wide linear range 0.01 to 13.18 mM and a comparable detection limit of 1.6 μM (3S/N). Gao et al. [20] prepared the Pt nanowires for hydrogen peroxide detection. The sensor displayed higher electrocatalytic response with a sensitivity of 171 μA mM⁻¹ cm⁻² and linear dynamic range up to 35 mM.

This work reveals that Ag NW arrays probably work as an advanced nanoelectrocatalyst for enhancing the detection of target molecules. In this paper, we developed a simple and rapid strategy for synthesizing Ag NW arrays via electrodeposition method by anodized aluminum oxide (AAO) template. The length of Ag NW arrays could be controlled by electrodeposition time. The Ag NW arrays (about 250nm length) were used for detecting H₂O₂. The proposed sensor had a high sensitivity excellent selectivity, and quick response to H₂O₂.

2. EXPERIMENTAL

2.1 Materials and reagents

High-purity aluminum foils (99.999%), H₂O₂ (30%), chromic trioxide (99%), acetone (99.5%), phosphoric acid (85%), and SnCl₄·5H₂O were purchased from the Guangzhou Chemical Reagents Company (Guangzhou, China). K₃Fe(CN)₆ and K₄Fe(CN)₆ were purchased from Aldrich.

$\text{NH}_4[\text{Ag}(\text{S}_2\text{O}_3)]$ was obtained from the Hongkong Yuhua Noble Metal Chemical Engineering Electroplating Company (Hongkong, China). All chemicals were of analytical grade and were used without further purification. All solutions were prepared with double-distilled water.

2.2 Apparatuses

A PARSTAT 2273 electrochemical workstation (Princeton, USA) was used for amperometry measurements and cyclic voltammetry measurements at 25 °C. Pt electrode was employed as counter and Ag/AgCl (saturated KCl) was used as reference electrodes. Scanning electron microscope analysis was performed with a Hitachi S-5200.

2.3 Preparation of Ag NW array electrodes

A glassy carbon electrode (GCE) was polished and thoroughly cleaned. A piece of as-prepared AAO template in our laboratory [21] was attached to the polished surface of the GCE by epoxy curing agent. Electrodeposition was carried out in an aqueous solution containing $\text{NH}_4[\text{Ag}(\text{S}_2\text{O}_3)]$. The chosen pH value was 6.4. The Ag NW arrays electrode was prepared at -0.34 V. In the end, the Ag NW arrays electrodes were dipped into H_3PO_4 solution (10%) for 1 h to completely remove the AAO and then they were washed with distilled water several times. About 150, 250, 400, 600 and 750 nm length Ag NW arrays were obtained by setting deposition time at 5, 7, 10, 13 and 15 min, respectively.

3. RESULTS AND DISCUSSION

3.1 Characterization

Fig.1(A-E) show the SEM micrographs of Ag NW arrays after AAO template has been completely dissolved. We can see that the average diameter of the pores in AAO template is about 80 nm. The length of the nanowires in Fig.1(A), (B), (C), (D) and (E) was about 150, 250, 400, 600 and 750nm, respectively. Moreover, it could also be observed that the aggregation effect became more obvious with increasing the length of nanowires. This is because nanomaterials themselves have aggregation effect and, when nanowires are grown to a certain length, the adjacent nanowires are no longer well-isolated parallel strand on electrode substrate. Fig.1F shows the EDX analysis of the Ag NW arrays. The major peaks corresponded to Ag, indicating that the AAO template was removed and confirming the formation of Ag NW arrays.

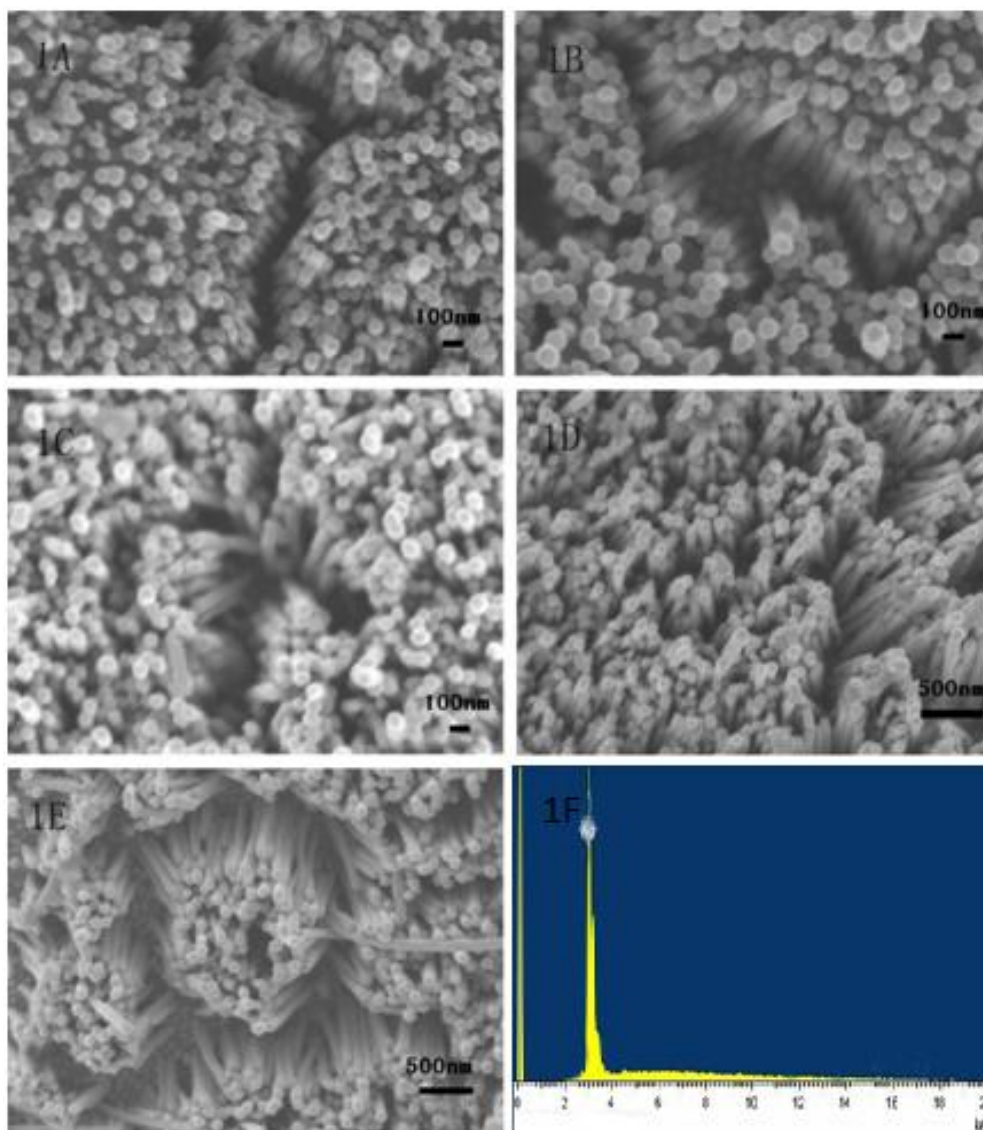


Figure 1. A-E. The SEM of Ag NW array; Fig. 1F EDX of Ag NW arrays

3.2 Electrochemistry of the sensor

Fig.2 (a)-(e) show the CV curves of different length Ag NW arrays modified electrodes for 1mM H_2O_2 in 0.1 M PBS solution. The reduction peak current was 41.9, 56.3, 38.7, 34.9 and 37.1 μA for about 150, 250, 400, 600 and 750nm length Ag NW arrays modified electrodes, respectively. About 250nm length nanowire showed the highest catalytic activity, which was due to the fact that with increasing the length of nanowire, its superficial area increases gradually and would accelerate H_2O_2 electron transfer on electrode surface. However, the aggregation effect of adjacent nanowires, in the mean time, also became more and more serious, which would decrease superficial area and reduce electron transfer interfaces. As a result, about 250 nm was the optimum length of Ag nanowire for preparing sensor towards H_2O_2 .

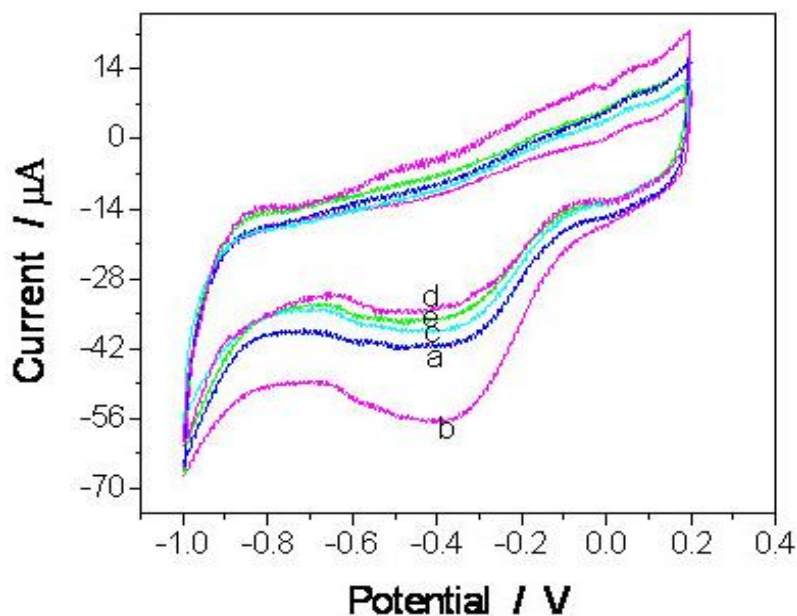


Figure 2. Cyclic voltammograms of 1 mM H_2O_2 in 0.1M PBS solution at about 150nm (a), 250 nm(b), 400 nm(c), 600 nm(d),750 nm(e) length Ag NW arrays electrode.

Fig.3 shows the CV curves of bare electrode, Ag film electrode and about 250 nm length Ag nanowire arrays electrode in a 0.1 M PBS solution in the presence of 1mM H_2O_2 .

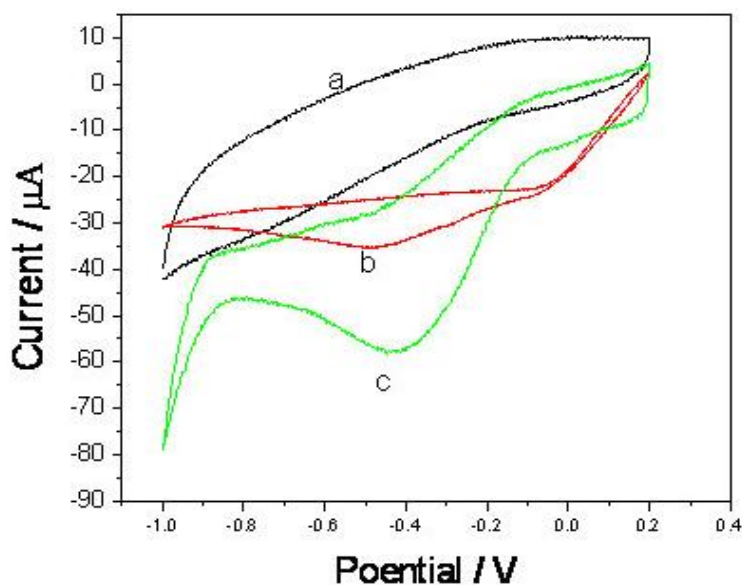


Figure 3. Cyclic voltammograms of 1 mM H_2O_2 in 0.1M PBS solution at bare electrode (a), Ag film electrode (b) and about 250nm length Ag NW arrays electrode(c).

No obvious peaks appeared on the bare electrode (Figs. 3a). This phenomenon indicated that the bare GCE showed poor electrocatalytic activity toward the reduction of H_2O_2 . A weak current peak (35.1 μA) was observed on the Ag film modified electrode at -0.47 V (Figs.3b) which could be

attributed to the reduction of H_2O_2 . On the other hand, about 250 nm length Ag nanowire arrays electrode exhibited a remarkable catalytic current peak ($57.4\mu\text{A}$) at -0.43V which indicating that Ag NW arrays could greatly increase the catalytic current toward the reduction of H_2O_2 , this was important for improving sensor sensitivity.

Fig. 4 shows the CVs of the proposed sensor in 0.1 M PBS solution in the presence of 5 mM H_2O_2 . The scan rate was 20, 40, 100, 140, 170, 200 and 250 mV/s, respectively. The peak current versus the square root of the scan rate (inserted in Fig. 4) exhibited a linear relationship ($R= 0.9977$), indicating a diffusion controlled electrode process.

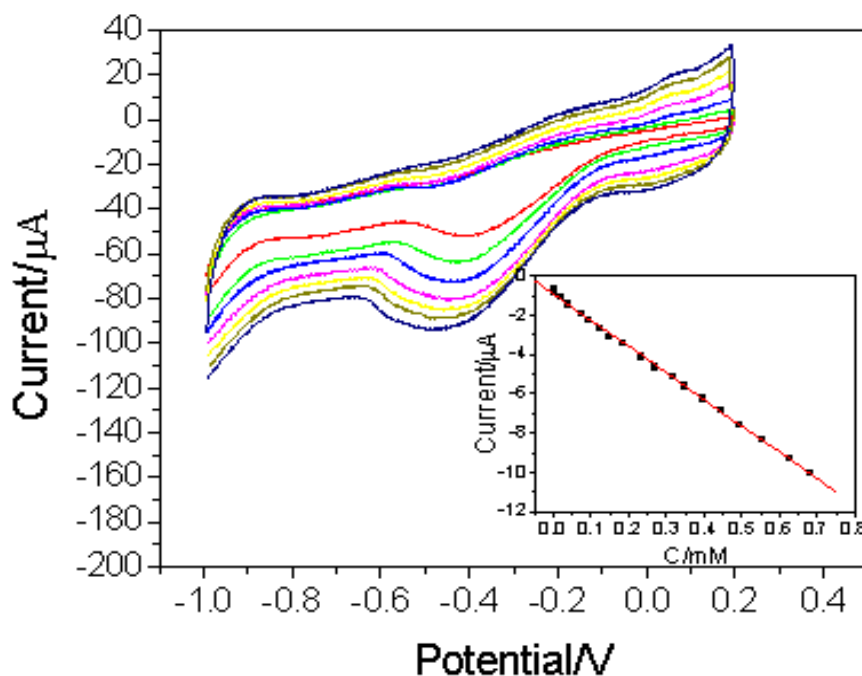


Figure 4. Cyclic voltammograms of 5 mM H_2O_2 in 0.1M PBS solution on about 250nm length Ag NW arrays electrode with different scan rates (inset: the relation of the anodic peak current for square root of scan rate).

Fig. 5 shows the amperometric response of Ag NW arrays electrode for the addition of different H_2O_2 concentrations into a continuous stirring 0.1M PBS solution at applied potential of -0.4V . The sensor responded quickly and could reach a steady state within 3s even though very low concentration H_2O_2 was added into solution, indicating Ag NW arrays exhibited excellent bio-electrocatalytic activity to H_2O_2 with a wide linear range (1 to $750\mu\text{M}$) ($R=0.999$), low detection limit ($0.28\mu\text{M}$) ($S/N=3$). The comparison of this sensor with various other nonenzymatic H_2O_2 sensor [5,16,18-19, 22-25] was listed in Table 1 which demonstrated that this proposed method has the comparable low detection limits and wide linear ranges for determination.

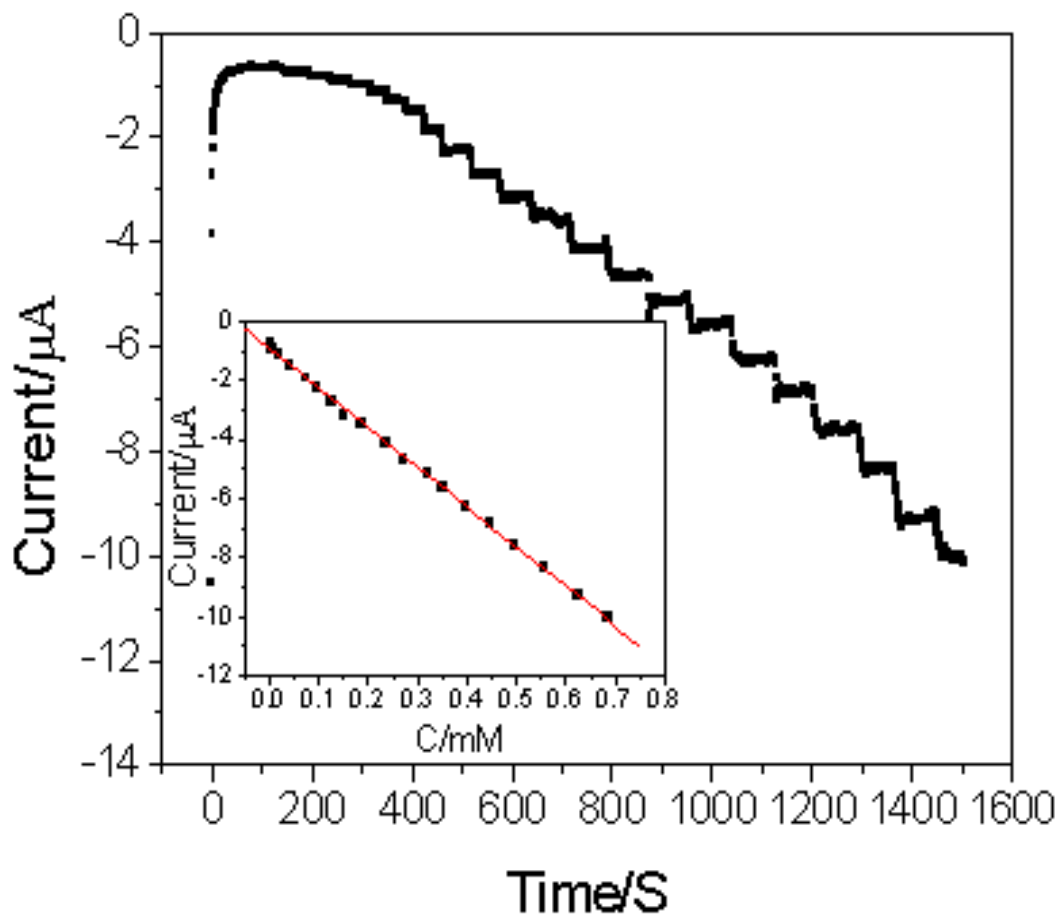


Figure 5. Current-time response of the sensor for successive addition of $0.01\text{ M H}_2\text{O}_2$ in 0.1 M PBS solution. The applied potential is -0.4 V . (inset: the calibration curve of the amperometric response).

Table 1 Comparison of various nonenzymatic H_2O_2 sensor

Nonenzymatic H_2O_2 sensor	Linear range (mM)	Detection limit (μM)	Reference
$\text{AgNPs-PPyCs}^{\text{a}}$ /GCE	0.1-90	1.05	[5]
AgNPs^{b} /MWCNTs-IL ^c /GCE	0.1-260	4	[16]
$\text{PdNP/AuNAE}^{\text{d}}$	-	5	[18]
CuO-SiNWs /GCE	0.01-13.18	1.6	[19]
n-Ag/GCE	0.05-6.5	27	[22]
PVP-Ag NWs ^e /GCE	0.02-3.6	2.3	[23]
Graphene-AgNPLs ^f /GCE	0.02-10	3	[24]
MnO_2 -Ag hybrid nanowire/GCE	0.1-4	0.24	[25]
Ag NWs arrays/GCE	0.001-0.75	0.28	This work

^aPPyCs: polypyrrole colloids; ^bNP: nanoparticles; ^cIL: ionic liquid; ^dAuNAE: gold nanowire array electrode.; ^eNWs: nanowires; ^fNPLs: nanoplates;

3.3 Sensor selectivity

As is known, some coexist electroactive biomolecules (UA, DA, glucose, etc.) generally show serious interference for electrochemical detection of H_2O_2 , which limit the real application of the sensor. Herein, it is essential to investigate the interferences introduced by common electrochemically active interferences during H_2O_2 detection. Fig 6 shows amperometric responses of the sensor to successive additions of 1mM H_2O_2 , 5mM of AA, 5mM of UA, 5mM of glucose, and 1mM H_2O_2 at an applied potential of -0.4 V. No obvious current changes were observed after adding AA, UA and glucose. Hence, at -0.4V, this sensor exhibited higher electrocatalytic activity towards H_2O_2 while AA, UA and glucose show negligible interference to H_2O_2 detection.

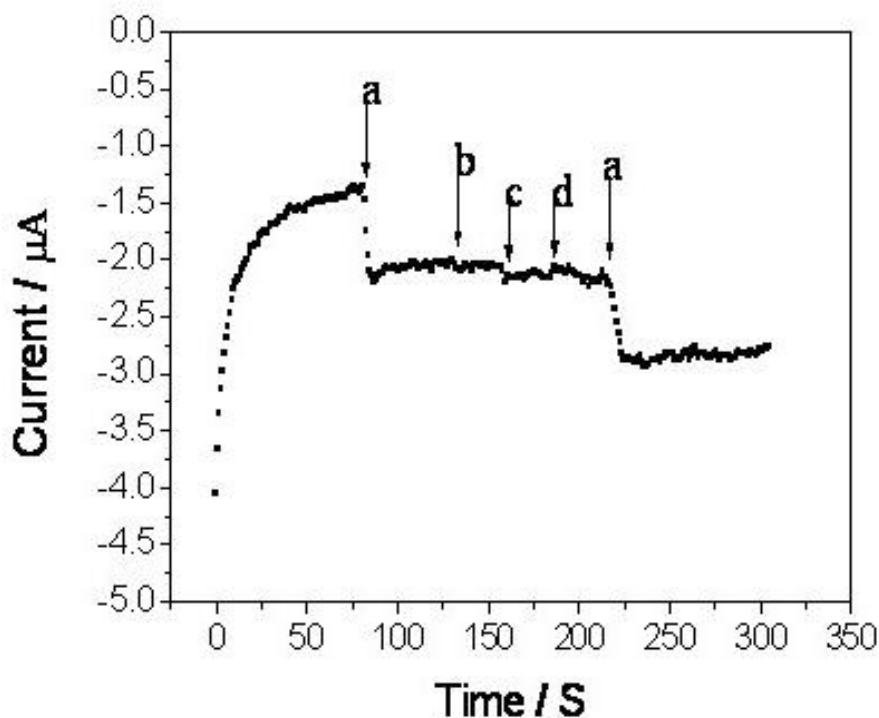


Figure 6. Amperometric response of about 250 nm length Ag NW arrays electrode to (a) 1 mM H_2O_2 , (b) 1 mM AA, (c) 1 mM UA and (d) 1 mM glucose in 0.1 M PBS solution. The applied potential is -0.4 V

3.4 Reproducibility and stability of the sensor

To characterize the repeatability of the sensor, successive determinations of H_2O_2 were carried out. The relative standard deviation (RSD) of the sensor response to 1 mM H_2O_2 was 1.8% for 10 successive measurements. Furthermore, when ten parallel modified electrodes were employed in the same solution, the relative standard deviations for H_2O_2 detection was 6.0%. The results suggested that the sensor has good repeatability and reproducibility. The electrode was kept at 4 °C and, the current keep 90.7% of the initial current after 7 days. The current still keep more than 85% of its initial current after 2 months, indicating that the sensor has a very stable and long life.

4. CONCLUSIONS

This work revealed that prepared Ag NW arrays using the template method are promising electrocatalysts for H₂O₂. The reported H₂O₂ sensor worked without using enzyme/mediator as an electron-transfer element. Electrochemical investigation was performed for about 150, 250, 400, 600 and 750 nm length Ag NW arrays modified electrodes in 1mM H₂O₂ solution. It could be found that about 250 nm length Ag NW electrode exhibited the highest catalytic activity. Moreover, the H₂O₂ sensor could detect H₂O₂ in the presence of AA, UA, and glucose. In addition, the H₂O₂ sensor exhibited a fast response time, high sensitivity, and a wide linear range.

ACKNOWLEDGEMENTS

We would like to thank the National Natural Science Foundation of China (No. 21375016, No.21475002), the Natural Science Foundations of Guangdong Province (No.S2013010014324).

References

1. J. C. Yuan and A. M. Shiller, *Anal. Chem.*, 71(1999) 975.
2. F. R. P. Rocha, E. R. Torralba, B. F. Reis, A. M. Rubio and M. D. I. Guardia, *Talanta*, 67(2005)673.
3. J. Odo, M. Inoguchi, S. Ohira, S. Tsukikawa, M. Aramaki, S. Matsuhama, M. Taito and A. Takayama, *Anal. Sci.*, 29(2013)1041.
4. S. M. Steinberg, *Environ. Monit. Assess.*, 185 (2013)3749.
5. X.Y. Qin, W. B. Lu, Y. L. Luo, G. H. Chang and X. P. Sun, *Electrochem. Commun.*, 13(2011)785.
6. L. A. Ticha, P. G. L. Baker, H. S. Abbo, S. J. J. Titinchi and E. I. Iwuoha, *Int. J. Electrochem. Sci.*, 12(2014)7335.
7. M. Shamsipur, M. Asgari, M. F. Mousavi and R. Davarkhah, *Eletroanalysis*, 2(2012)357.
8. J. Zhang, J. Li, F. Yang, B. L. Zhang and X. R. Yang, *J. Electroanal. Chem.* 638(2010)173.
9. W. Wang, Y. B. Xie, C. Xia, H. X. Du and F. Tian, *Microchim Acta*, 181(2014):1325.
10. P. H. C. Camargo, Y. Xiong, L. Ji, J. M. Zuo and Y. J. Xia, *J. Am. Chem. Soc.* 129(2007)15452.
11. Y. Xia, Y. Xiong, B. Lim and S. E. Skrabalak, *Angew. Chem. Int. Ed.* 48(2008)60.
12. J. Yan, S. Liu, Z. Q. Zhang, G. W. He, P. Zhou, H. Y. Liang, L. L. Tian, X. M. Zhou and H. J. Jiang, *Colloid. Surface. B.*, 111(2013)392.
13. R. Y. Li, J. J. Zhang, Z. P. Wang, Z. J. Li, J. K. Liu, Z. G. Gu, G. G. L. Wang, *Sens. Actuators, B: Chem.*, 208(2015)421.
14. Y. L. Du, X. Gao, X. L. Ye, Z. X. Zheng, Q. L. Feng, C. M. Wang and K. F. Wu, *Sens. Actuators, B: Chem.*, 203(2014)926.
15. S. Thatai, P. Khurana, S. Prasad, D. Kumar, *Microchem. J.*, 113(2014)77.
16. X. Y. Li, Y. X. Liu, L. C. Zheng, M. J. Dong, Z. H. Xue, X. Q. Lu and X. H. Liu, *Electrochim. Acta*, 113(2013)170.
17. W. B. Lu, Y. L. Luo, G. H. Chang and X. P. Sun, *Biosens. Bioelectron.*, 26(2011)4791.
18. M. Jamal, M. Hasan, A. Mathewson and K. M. Razeeb, *J. Electrochem. Soc.*, 159(2012): 825.
19. J. F. Huang, Y. H. Zhu, H. Zhong, X. L. Yang and C. Z. Li, *ACS Appl. Mater. Interfaces*, 6(2014)7055.
20. F. Gao, Z. Y. Li, D. J. Ruan and Z. Y. Gu, *J Nanosci. Nanotechno.*, 14(2014)6599.
21. C. W. Xu, H. Wang, P. K. Shen and S. P. Jiang, *Adv. Mater.*, 17(2007)4256.
22. J. B. Raouf, R. Ojani, E. Hasheminejad, S. Rashid-Nadimi, *Appl. Surf. Sci.*, 258 (2012) 2788.

23. X. J. Yang, J. Bai, Y. H. Wang, X. E. Jiang and X.Y. He, *Analyst*, 137 (2012) 4362.
24. L. J. Zhong, S. Y. Gan, X. G. Fu, F. H. Li, D. X. Han, L. P. Guo and L. Niu, *Electrochim. Acta*, 89(2013)222.
25. Q. Han, P. J. Ni, Z. R. Liu, X. T. Dong, Y. Wang, Z. Li, Z. L. Liu, *Electrochem. Commun.*, 38(2014)110.

© 2015 The Authors. Published by ESG (www.electrochemsci.org). This article is an open access article distributed under the terms and conditions of the Creative Commons Attribution license (<http://creativecommons.org/licenses/by/4.0/>).